

This is the accepted manuscript made available via CHORUS. The article has been published as:

Universal entanglement spectra in critical spin chains

Rex Lundgren, Jonathan Blair, Pontus Laurell, Nicolas Regnault, Gregory A. Fiete, Martin Greiter, and Ronny Thomale

Phys. Rev. B **94**, 081112 — Published 26 August 2016

DOI: [10.1103/PhysRevB.94.081112](https://doi.org/10.1103/PhysRevB.94.081112)

Universal entanglement spectra in critical spin chains

Rex Lundgren,¹ Jonathan Blair,¹ Pontus Laurell,¹ Nicolas Regnault,^{2,3}

Gregory A. Fiete,¹ Martin Greiter,⁴ and Ronny Thomale⁴

¹*Department of Physics, The University of Texas at Austin, Austin, Texas 78712, USA*

²*Department of Physics, Princeton University, Princeton NJ 08544, USA*

³*Laboratoire Pierre Aigrain, Ecole Normale Supérieure-PSL Research University,
CNRS, Université Pierre et Marie Curie-Sorbonne Universités,*

Université Paris Diderot-Sorbonne Paris Cité, 24 rue Lhomond, 75231 Paris Cedex 05, France

⁴*Institute for Theoretical Physics, University of Würzburg, D-97074 Würzburg, Germany*

We advocate that in critical spin chains, and possibly in a larger class of 1D critical models, a gap in the momentum-space entanglement spectrum separates the universal part of the spectrum, which is determined by the associated conformal field theory, from the non-universal part, which is specific to the model. To this end, we provide affirmative evidence from multicritical spin chains with low energy sectors described by the $SU(2)_2$ or the $SU(3)_1$ Wess-Zumino-Witten model.

Introduction.—Quantum entanglement has become a key concept in contemporary condensed matter physics. This is due in part to its ability to probe intrinsic topological order^{1–3}. Consider a density matrix, ρ , represented by the projector onto a many-body ground state. If the associated Hilbert space is partitioned into two non-overlapping regions A and B , two possible ways to characterize the entanglement between the regions A and B are the entanglement entropy (EE) and the entanglement spectrum (ES), which is obtained from the reduced density matrix $\rho_A = \text{Tr}_B \rho$. The EE is given by $S_A = -\text{Tr}(\rho_A \ln \rho_A)$, and the ES is defined as the spectrum of the entanglement Hamiltonian $H_E = -\ln \rho_A$ ⁴. By definition, EE and ES depend on the chosen basis to partition (cut) the many-body Hilbert space. To resolve bulk and edge features of topological order, some form of spatial cut^{4–10} (along with a particle cut^{11,12}) is the predominantly used choice. This works well in systems with a bulk energy gap and hence an associated length scale. Upon partitioning, the ES then mimics the physical energy spectrum of edge states along the cut⁷. In particular, a set of universal entanglement levels, i.e. eigenvalues of H_e , related to physical edge states can be identified as distinct from generic entanglement levels through the entanglement gap (EG), which can be employed to investigate topological adiabaticity (whether two states are topologically connected) using *just the ground state wavefunction*⁵. The spatial EG evolves in a way similar to the physical bulk gap of the topologically ordered phase, even though bulk gap closures occur at points of parameter space different from EG (physically, this is because physical properties of a system are determined by $\rho_A = e^{-H_e}$, i.e. H_e at a fictitious finite temperature, while the EG captures the low energy properties of H_e)¹³.

In order to understand the universal properties of entanglement in critical systems, a spatial cut is not always a preferable choice^{14–17}. Due to the absence of an energy gap, there will not be an appreciable concentration of entanglement localized along the cut. Furthermore, for geometries where a spatial cut induces multiple edges, such as a ring or torus, the entanglement

modes couple between the edges, and complicate the resolution of individual modes. Instead, a momentum basis appears promising to detect universal critical entanglement profiles. The momentum-space ES was first introduced for spin-1/2 chains¹⁸. There, the notion of momentum relates to the Fourier transform of individual spin flip operators, and the total spin flip momentum, M_A , of spin flips in momentum region A provides an approximate quantum number of ρ_A . The spin fluid phase around the Heisenberg spin chain was found to exhibit a large EG (the EG is infinite at the spin-half Haldane-Shastry point^{19,20}) and a counting of entanglement levels below the EG which identify the low energy field theory (a massless $U(1)$ boson) of the Heisenberg point. Interestingly, the same counting, along with an EG, is also seen in the (conformal limit construction) ES of the Laughlin state⁵. This similarity can be understood by observing that the Haldane-Shastry model and Laughlin state have the same polynomial structure¹⁸. The momentum-space ES has been subsequently explored in the XXZ spin-1/2 chain²¹, spin-ladders^{22,23}, and disordered systems^{24,25}. Momentum-space entanglement has also been employed in the context of high-energy physics such as interacting quantum field theories²⁶ and D -branes in string theory^{27,28}. As an overarching principle, the momentum EG, along with the *universal* entanglement levels below it, require an interpretation different from the spatial cut. In a finite spin chain with no length scale, except for the UV lattice cutoff $1/a$ and IR chain length cutoff $1/L$, the EG cannot be directly related to a microscopic scale. As a central conjecture emerging from previous work, the EG separates the non-universal part of the ES above it from the universal part below it, which is determined by the associated conformal field theory (CFT). We refer to this assumption as the universal bulk entanglement conjecture (UBEC).

In this Rapid Communication, we elevate this conjecture to a general principle, as we confirm it for several critical spin chains with different, intricate field theories. In particular, we analyze the momentum-space ES of several critical spin-1 chains, including the

Takhtajan-Babujian (TB) point^{29,30} and the Uimin-Lai-Sutherland (ULS) point^{31–33} associated with an $SU(2)_2$ and an $SU(3)_1$ Wess-Zumino-Witten (WZW) field theory, respectively. Both are critical points in the bilinear-biquadratic spin-1 model. (For a detailed complementary study of the real-space ES see Ref.¹⁶.) Our work generalizes the connection between the momentum-space ES of critical spin-chains and ES of FQH states beyond Laughlin states. We pursue our analysis in two steps. First, we identify fine-tuned models related to $SU(2)_2$ and $SU(3)_1$ WZWs, which exhibit an infinite EG, relating to an extensive multiplicity of the eigenvalue zero in ρ_A . For $SU(3)_1$ WZW, this is the $SU(3)$ symmetric generalization of the Haldane-Shastry model^{19,20,34}. For $SU(2)_2$ WZW, this is the Pfaffian spin chain^{35,36}. Second, we turn to the TB and ULS point, where we find a finite EG along with a precise matching of energy levels for the universal entanglement content as compared to their associated infinite-EG models.

$SU(3)_1$ WZW theory.—Starting from the spin-1/2 fluid phase where the universal behavior we advocate was first observed for an $SU(2)_1$ WZW theory, one way of generalization is the enlargement of the internal symmetry group. The low energy sector of the ULS model is described by $SU(3)_1$ WZW theory with central charge $c = 2$. Equivalently, $SU(3)_1$ WZW can be thought of as two gapless free bosonic field theories, each with unit central charge³⁷. In terms of $S = 1$ spin operators, the Hamiltonian is given by $H_{\text{ULS}} = \sum_{\alpha=1}^N \mathbf{S}_\alpha \mathbf{S}_{\alpha+1} + \sum_{\alpha=1}^N (\mathbf{S}_\alpha \mathbf{S}_{\alpha+1})^2$. Periodic boundary conditions (PBCs) are implemented by placing the sites on a unit circle embedded into the complex plane, with site coordinates $\eta_\alpha = \exp(i2\pi\alpha/N)$, $\alpha \in \{1, \dots, N\}$. Due to its enlarged symmetry, the ULS model can be recast (up to a constant) in terms of $SU(3)$ spin vectors¹⁶,

$$H_{\text{ULS}} = \sum_{\alpha=1}^N \mathbf{J}_\alpha \cdot \mathbf{J}_{\alpha+1}, \quad (1)$$

where $\mathbf{J}_\alpha = \frac{1}{2} \sum_{\sigma\tau} c_{\alpha\sigma}^\dagger \boldsymbol{\lambda}_{\sigma\tau} c_{\alpha\tau}$ denotes the $SU(3)$ spin vector on site α , $\boldsymbol{\lambda}_{\sigma\tau}$ is a vector consisting of the eight Gell-Mann matrices, $c_{\alpha\sigma}^\dagger$ is an electron creation operator (with color σ) on site α , and $\tau, \sigma \in \{r, g, b\}$. We contrast model (1) with the $SU(3)$ Haldane-Shastry model

$$H_{\text{HS}}^{SU(3)} = \frac{2\pi^2}{N^2} \sum_{\alpha \neq \beta}^N \frac{\mathbf{J}_\alpha \cdot \mathbf{J}_\beta}{|\eta_\alpha - \eta_\beta|^2}, \quad (2)$$

where $|\eta_\alpha - \eta_\beta|$ is the chord distance along the ring.

In order to perform a momentum cut for the finite size ground state of (1) and (2), we first need to specify the operators which span the Hilbert space of the spin chain. In analogy to the spin flip operators, S_α^+ , S_α^- , which are formed by the adjoint representation of $SU(2)$, we have the color flip operators $e_\alpha^{\sigma\tau} = c_{\alpha\sigma}^\dagger c_{\alpha\tau}$ for $SU(3)$. Assuming $N = 0 \bmod 3$, the ground states of (1) and (2)

will be $SU(3)$ singlets due to a generalized interpretation of the Marshall theorem³⁸. We write

$$|\psi_0\rangle = \sum_{\{z;w\}} \psi_0[z;w] e_{z_1}^{\text{bg}} \dots e_{z_{N/3}}^{\text{bg}} e_{w_1}^{\text{rg}} \dots e_{w_{N/3}}^{\text{rg}} |0_g\rangle, \quad (3)$$

where the sum extends over all possible ways of distributing the positions $[z] \equiv z_1, \dots, z_{N/3}$ of the blue (and $[w] \equiv w_1, \dots, w_{N/3}$ of the red) particles. $|0_g\rangle = \prod_{\alpha=1}^N c_{\alpha g}^\dagger |0\rangle$ is a reference state consisting only of green particles, on which we act with the color flip operators e_α^{bg} and e_α^{rg} . We define the momentum space operators \tilde{e}_p^{bg} and \tilde{e}_q^{rg}

$$e_\alpha^{\text{bg}} = \frac{1}{\sqrt{N}} \sum_{p=1}^N \bar{\eta}_\alpha^p \tilde{e}_p^{\text{bg}}, \quad e_\beta^{\text{rg}} = \frac{1}{\sqrt{N}} \sum_{q=1}^N \bar{\eta}_\beta^q \tilde{e}_q^{\text{rg}}, \quad (4)$$

where $p, q \in \{1, \dots, N\}$ are integer spaced momentum indices. Substitution of (4) into (3) yields

$$|\psi_0\rangle = \sum_{\{p;q\}} \tilde{\psi}_0[p;q] \tilde{e}_{p_1}^{\text{bg}} \dots \tilde{e}_{p_{N/3}}^{\text{bg}} \tilde{e}_{q_1}^{\text{rg}} \dots \tilde{e}_{q_{N/3}}^{\text{rg}} |0_g\rangle, \quad (5)$$

$$\tilde{\psi}_0[p;q] = \sum_{\{z;w\}} \psi_0[z;w] \bar{z}_1^{p_1} \dots \bar{z}_{N/3}^{p_{N/3}} \bar{w}_1^{q_1} \dots \bar{w}_{N/3}^{q_{N/3}}. \quad (6)$$

Note that while there trivially is a hard-core constraint for the color flip operators in real space, there is no such condition in momentum space. This significantly enlarges the number of basis states. For our purposes, it is best to write the ground state in a momentum space occupation number basis,

$$|\psi_0\rangle = \sum_{\{n;m\}} \tilde{\phi}_0[n;m] |n_1, \dots, n_N; m_1, \dots, m_N\rangle, \quad (7)$$

where n_p (m_q) is the number of times momentum index p (q) for color flips from green to blue (red) appears in (5). The ket in (7) is hence given by

$$|n_1 \dots; m_1, \dots\rangle = \prod_{p=1}^N \frac{(\tilde{e}_p^{\text{bg}})^{n_p}}{\sqrt{n_p!}} \prod_{q=1}^N \frac{(\tilde{e}_q^{\text{rg}})^{m_q}}{\sqrt{m_q!}} |0_g\rangle. \quad (8)$$

We arrive at Eq. (7) after obtaining the real space ground state via exact diagonalization. Due to the exponential numerical cost of the many-particle Fourier transform, the maximal size we are able to reach is $N = 15$.

We are now prepared to calculate the momentum ES for (1) and (2)³⁹. Assuming N odd, we partition momentum into regimes

$$A = \{p | p \leq \frac{N+1}{2}\} \otimes \{q | q \leq \frac{N+1}{2}\} \quad (9)$$

and

$$B = \{p | p > \frac{N+1}{2}\} \otimes \{q | q > \frac{N+1}{2}\}. \quad (10)$$

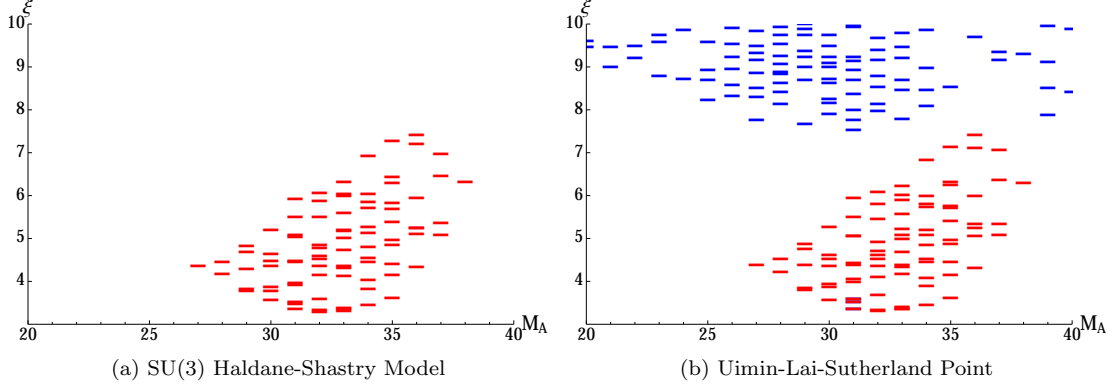


FIG. 1. (color online) (a) ES of Eq. (2) and (b) ES of the ULS point for $(N, N_A) = (15, 6)$, 3 red and 3 blue particles. At the ULS point, generic entanglement levels (blue) are separated by a finite EG from the universal entanglement levels (red). The eigenvalues, ξ , are plotted versus the total momentum of region A . Throughout this work, ρ_A is normalized such that $\text{Tr } \rho_A = 1$ for each N_A . The universal entanglement in (a) and (b) matches the counting of $\text{SU}(3)_1$ WZW theory, supporting the UBEC.

Region A and B are decomposed in terms of total momentum, $M = M_A + M_B$, and particle number, $N = N_A + N_B$, which are given by

$$N_{A/B} = \sum_{p \in A/B} n_p + \sum_{q \in A/B} m_q, \quad (11)$$

and

$$M_{A/B} = \sum_{p \in A/B} n_p p + \sum_{q \in A/B} m_q q. \quad (12)$$

The crystal momentum is given by $M_{A/B}^c = M_{A/B} \bmod N$, and is always an exact quantum number of $\rho_{A/B}$. In general, however, even $M_{A/B}$ is a good approximate quantum number. For an $N = 12$ ground state of (1), more than 99% of the total amplitude resides in the $M = \frac{N^2}{3}$ sector and less than 1% in all other sectors. It is a central observation that M (and $M_{A/B}$) is a good approximate quantum number as long as the internal spin symmetry is unbroken or only weakly broken^{18,21}.

The ground state of (2) retains $M_{A/B}$ as an *exact* quantum number. Fig. 1a displays its $(N, N_A) = (15, 6)$, $N_{A,r} = N_{A,b} = 3$ sector of H_E with spectral levels denoted by ξ . We observe a large degeneracy of entanglement levels at infinity, corresponding to eigenvalues zero of ρ_A . The counting 1, 2, 5 of the ES levels from left to right matches the state counting of two gapless $\text{U}(1)$ bosons until we reach a finite size limit. All properties above are understood on analytic footing: For (2), $\psi_0^{\text{HS}}[z; w]$ is given by⁴⁰

$$\psi_0^{\text{HS}}[z; w] = \prod_{i < j}^{N/3} (z_i - z_j)^2 (w_i - w_j)^2 \cdot \prod_{i,j=1}^{N/3} (z_i - w_j) \prod_{i=1}^{N/3} z_i w_i. \quad (13)$$

Note that one can write the ground state in terms of color flip operators for any pair of colors (up to a minus sign)⁴¹.

By virtue of a momentum-conserving orbital squeezing relation between Fock states of non-zero weight, Eq. (13) has all of its weight in the sector $M = N^2/3$. To understand this, note that (13), in its polynomial form, is equivalent to the spin-singlet bosonic Halperin-(221) fractional quantum Hall (FQH) state⁴² with filling fraction $\nu = \frac{2}{3}$. Vice versa, the bosonic Halperin-(221) state exhibits $\text{SU}(3)$ symmetry⁴³. As the Halperin-(221) state obeys certain squeezing properties^{44,45}, so does (13). In terms of critical theories, (2) is special in the sense that the finite size ground state does not contain corrections as compared to the thermodynamic field theoretical content of entanglement.

Turning to the ES at the ULS point (1) in Fig. 1b, we observe an EG present for all M_A , which separates the non-universal components at higher ξ from universal levels which match with the entanglement levels of (2). As one increases the system size, the relative importance of non-universal entanglement levels would decrease while the universal entanglement weight⁴⁶ becomes successively dominant and stays separated from non-universal levels through the EG. It implies that the UBEC also holds for critical spin chains described by $\text{SU}(3)_1$ WZW theory.

$\text{SU}(2)_{k=2}$ WZW theory.—Another way to explore the reach of the UBEC is the extension to higher level $k > 1$ Wess-Zumino terms in the field theory description of critical spin chains. Higher k links to multi-critical points which in general do not represent gapless spin fluid phases, but rather phase transition points⁴⁷. For $\text{SU}(2)_2$ WZW theory, several model instances have been found for spin-1 chains such as the TB spin chain, $H_{\text{TB}} = \sum_{\alpha=1}^N \mathbf{S}_\alpha \mathbf{S}_{\alpha+1} - \sum_{\alpha=1}^N (\mathbf{S}_\alpha \mathbf{S}_{\alpha+1})^2$. An analytic lattice realisation of $\text{SU}(2)_2$ WZW theory has been found

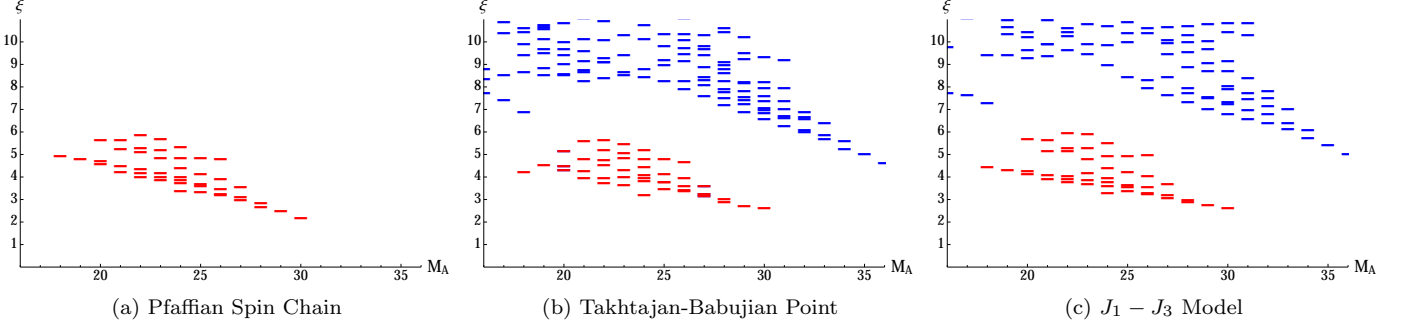


FIG. 2. (color online) (a) ES of Eq. (14), (b) ES of the TB point, and (c) ES of the $J_1 - J_3$ model for $(N, N_A) = (12, 6)$. In (b) and (c), the universal (red) and non-universal (blue) entanglement levels are separated by a finite EG. For (a)-(c), the counting of the universal levels matches the counting of $SU(2)_2$ WZW theory, consistent with the UBEC.

for the Pfaffian spin chain^{35,48},

$$H^{\text{Pf}} = \frac{2\pi^2}{N^2} \left[\sum_{\alpha \neq \beta}^N \frac{\mathbf{S}_\alpha \mathbf{S}_\beta}{|\eta_\alpha - \eta_\beta|^2} - \frac{1}{20} \sum_{\substack{\alpha, \beta, \gamma \\ \alpha \neq \beta, \gamma}}^N \frac{(\mathbf{S}_\alpha \mathbf{S}_\beta)(\mathbf{S}_\alpha \mathbf{S}_\gamma) + (\mathbf{S}_\alpha \mathbf{S}_\gamma)(\mathbf{S}_\alpha \mathbf{S}_\beta)}{(\bar{\eta}_\alpha - \bar{\eta}_\beta)(\eta_\alpha - \eta_\gamma)} \right]. \quad (14)$$

The low-energy theory is described by a massless bosonic and Majorana field consistent with $c = 1 + 0.5$ ³⁶. Numerical evidence for $SU(2)_2$ critical behaviour has been independently found for a truncated version of (14),

$$H^{J_1-J_3} = \left[\sum_{\alpha=1}^N \mathbf{S}_\alpha \mathbf{S}_{\alpha+1} + \frac{J_3}{J_1} [(\mathbf{S}_{\alpha-1} \mathbf{S}_\alpha)(\mathbf{S}_\alpha \mathbf{S}_{\alpha+1}) + \text{h.c.}] \right], \quad (15)$$

at $J_3/J_1 \approx 0.11$, with a central charge $c = 1.5$ ⁴⁹.

The singlet ground state of any spin-1 chain of length N (N even) reads

$$|\psi_0^{S=1}\rangle = \sum_{\{z\}} \psi_0(z_1, \dots, z_N) \tilde{S}_{z_1}^+ \dots \tilde{S}_{z_N}^+ |-1\rangle_N, \quad (16)$$

where the sum extends over all possible configurations of N spin-flip operators (allowing for at most two spin flips on the same site), $|-1\rangle_N = \otimes_{i=1}^N |s_i^z = -1\rangle$ is the vacuum with all spins in the $s^z = -1$ state, and $\tilde{S}_\alpha^+ = \frac{1}{2}(S_\alpha^z + 1)S_\alpha^+$ is a renormalized spin flip operator⁵⁰. They are the natural choice to unify a Pfaffian polynomial of spin flip coordinates with the singlet property of the resulting wave function, such that the ground state of (14) yields

$$\psi_0^{\text{Pf}}(z_1, \dots, z_N) = \text{Pf} \left(\frac{1}{z_i - z_j} \right) \prod_{i < j}^N (z_i - z_j) \prod_{i=1}^N z_i, \quad (17)$$

where $\text{Pf}(1/(z_i - z_j)) = \mathcal{A}[1/(z_1 - z_2) \dots 1/(z_{N-1} - z_N)]$. An alternative construction of (17) is given by the

symmetrization over two $S=1/2$ Haldane-Shastry chain states^{50,51}. We Fourier transform the spin-flip operators as

$$S_\alpha^+ = \frac{1}{\sqrt{N}} \sum_{q=1}^N \bar{\eta}_\alpha^q \tilde{S}_q^+, \quad \tilde{S}_q^+ = \frac{1}{\sqrt{N}} \sum_{\alpha=1}^N \eta_\alpha^q S_\alpha^+. \quad (18)$$

Substituting (18) into (16), we find

$$|\psi_0^{S=1}\rangle = \sum_{\{q\}} \tilde{\psi}_0(q_1, \dots, q_N) \tilde{S}_{q_1}^+ \dots \tilde{S}_{q_N}^+ |-1\rangle_N, \quad (19)$$

$$\tilde{\psi}_0(q_1, \dots, q_N) = \sum_{\{z\}} \psi_0(z_1, \dots, z_N) \bar{z}_1^{q_1} \dots \bar{z}_N^{q_N}. \quad (20)$$

From the Fourier transformed ground state, we obtain the momentum-space ES. We partition our system in two regions, A and B, by dividing the momentum-space occupation basis as $A = \{q | q < \frac{N}{2}\}$ and $B = \{q | q > \frac{N}{2}\}$. Each region is decomposed in terms of number of particles $N = N_A + N_B = \sum_{q=1}^N n_q$ and total momentum $M = M_A + M_B = \sum_{q=1}^N n_q q$, where n_q denotes the occupation number of a given momentum q . As previously seen for the $SU(3)$ case, $M^c = M \bmod N$ is an exact quantum number, while M in general is not. By virtue of being a squeezing state, however, (17) has all of its weight in the sector $M = N^2/2$. Similarly, it turns out that $M = N^2/2$ is the strongly preferred sector for the TB model and the $J_1 - J_3$ model as well, rendering M_A a good approximate quantum number. (For instance, the $N = 10$ TB ground state has 94% of its total weight in the $M = 50$ sector.)

Fig. 2a depicts the $(N, N_A) = (12, 6)$ ES of (17) in comparison to the ES of the TB and $J_1 - J_3$ ground state in Fig. 2b and Fig. 2c, respectively. For all ES, we observe a matching of universal levels which corresponds to counting $1, 1, 3, \dots$ of the low-lying entanglement levels from left to right. This corresponds to the energy levels of a boson and a Majorana fermion with anti-periodic boundary conditions⁵². For $N_A = 7$ (not shown), the observed counting is $1, 2, 4, \dots$, and as such also consistent

with the previous finding⁵³. In contrast, Fig. 2a shows no non-universal entanglement weight beyond the universal levels, *i.e.*, an extensive number of zero modes in ρ_A . This is due to the monomial equivalence between (17) and the bosonic Moore-Read state⁵⁴. Fig. 2b and Fig. 2c exhibit different non-universal entanglement weight, which is again separated from the universal weight by an EG, in agreement with the UBEC. Note that in analytically unresolved cases such as the model $J_3/J_1 \approx 0.11$ in $H_{J_1-J_3}$, the momentum entanglement fingerprint provides a particularly elegant tool to identify the critical theory.

The momentum-space ES also has some advantages over (bipartite) real-space entanglement measures used to identify CFTs. The real-space entanglement entropy ($\frac{c}{3} \ln L$ in a CFT⁵⁵) of (14), computed using the density matrix renormalization group algorithm, predicts $c = 1.46(2)$ ³⁶. While consistent with $c = \frac{3}{2}$, *our method confirms c exactly using only small system sizes*. The real-space ES reveals c through the distribution of entanglement levels¹⁴ and can be identified as a boundary CFT¹⁵. Still, as a tool for identifying c , it is limited by finite size effects⁵⁶.

Conclusions and Outlook.—At the example of critical spin-1 chains, we have provided evidence that the universal bulk entanglement conjecture for critical spin chains generically holds for $SU(N)_k$ Wess-Zumino-Witten theo-

ries. As a concrete example, one would expect to see an EG in the momentum-space ES (upon Fourier transforming the correct quantum operator) for $SU(N)_1$ Heisenberg models, which were constructed in Refs.^{57,58}, and their generalization to higher k ^{59,60}. It would also be interesting to investigate the anisotropic generalization of the TB point with the momentum-space ES⁶¹. From a broader perspective, our work highlights that entanglement spectra do not only provide universal fingerprints for topological phases, but also for critical systems.

Acknowledgments.—R.L. was supported by National Science Foundation (NSF) Graduate Research Fellowship award number 2012115499, a fellowship from the Office of Graduate Studies at The University of Texas at Austin, and NSF Grant No. DMR-0955778. P.L. and G.A.F. acknowledge financial support through NSF Grant No. DMR-1507621. N. R. was supported by the Princeton Global Scholarship. M.G. and R.T. are supported by DFG-SFB 1170. R.T. was supported by DFG-SPP 1458 and the ERC starting grant TOPOLECTRICS of the European Research Council (ERC-StG-Thomale-2013-336012). We acknowledge the Texas Advanced Computing Center (TACC) at The University of Texas at Austin for providing computing resources that have contributed to the research results reported within this paper. URL: <http://www.tacc.utexas.edu>

-
- ¹ X. G. Wen, *Phys. Rev. B* **40**, 7387 (1989).
 - ² A. Kitaev and J. Preskill, *Phys. Rev. Lett.* **96**, 110404 (2006).
 - ³ M. Levin and X.-G. Wen, *Phys. Rev. Lett.* **96**, 110405 (2006).
 - ⁴ H. Li and F. D. M. Haldane, *Phys. Rev. Lett.* **101**, 010504 (2008).
 - ⁵ R. Thomale, A. Sterdyniak, N. Regnault, and B. A. Bernevig, *Phys. Rev. Lett.* **104**, 180502 (2010).
 - ⁶ A. M. Läuchli, E. J. Bergholtz, J. Suorsa, and M. Haque, *Phys. Rev. Lett.* **104**, 156404 (2010).
 - ⁷ X.-L. Qi, H. Katsura, and A. W. W. Ludwig, *Phys. Rev. Lett.* **108**, 196402 (2012).
 - ⁸ R. Lundgren, Y. Fuji, S. Furukawa, and M. Oshikawa, *Phys. Rev. B* **88**, 245137 (2013).
 - ⁹ F. Pollmann, A. M. Turner, E. Berg, and M. Oshikawa, *Phys. Rev. B* **81**, 064439 (2010).
 - ¹⁰ X. Deng and L. Santos, *Phys. Rev. B* **84**, 085138 (2011).
 - ¹¹ M. Haque, O. Zozulya, and K. Schoutens, *Phys. Rev. Lett.* **98**, 060401 (2007).
 - ¹² A. Sterdyniak, N. Regnault, and B. A. Bernevig, *Phys. Rev. Lett.* **106**, 100405 (2011).
 - ¹³ A. Chandran, V. Khemani, and S. L. Sondhi, *Phys. Rev. Lett.* **113**, 060501 (2014).
 - ¹⁴ P. Calabrese and A. Lefevre, *Phys. Rev. A* **78**, 032329 (2008).
 - ¹⁵ A. M. Läuchli, ArXiv e-prints (2013), [arXiv:1303.0741](https://arxiv.org/abs/1303.0741) [cond-mat.stat-mech].
 - ¹⁶ R. Thomale, S. Rachel, B. A. Bernevig, and D. P. Arovas, *Journal of Statistical Mechanics: Theory and Experiment* **2015**, P07017 (2015).
 - ¹⁷ G. De Chiara, L. Lepori, M. Lewenstein, and A. Sanpera, *Phys. Rev. Lett.* **109**, 237208 (2012).
 - ¹⁸ R. Thomale, D. P. Arovas, and B. A. Bernevig, *Phys. Rev. Lett.* **105**, 116805 (2010).
 - ¹⁹ F. D. M. Haldane, *Phys. Rev. Lett.* **60**, 635 (1988).
 - ²⁰ B. S. Shastri, *Phys. Rev. Lett.* **60**, 639 (1988).
 - ²¹ R. Lundgren, J. Blair, M. Greiter, A. Läuchli, G. A. Fiete, and R. Thomale, *Phys. Rev. Lett.* **113**, 256404 (2014).
 - ²² R. Lundgren, V. Chua, and G. A. Fiete, *Phys. Rev. B* **86**, 224422 (2012).
 - ²³ R. Lundgren, *Phys. Rev. B* **93**, 125107 (2016).
 - ²⁴ I. Mondragon-Shem, M. Khan, and T. L. Hughes, *Phys. Rev. Lett.* **110**, 046806 (2013).
 - ²⁵ E. C. Andrade, M. Steudtner, and M. Vojta, *Journal of Statistical Mechanics: Theory and Experiment* **7**, 07022 (2014), [arXiv:1403.2599](https://arxiv.org/abs/1403.2599) [cond-mat.dis-nn].
 - ²⁶ V. Balasubramanian, M. B. McDermott, and M. Van Raamsdonk, *Phys. Rev. D* **86**, 045014 (2012).
 - ²⁷ L. A. Pando Zayas and N. Quiroz, *Journal of High Energy Physics* **2015**, 1 (2015).
 - ²⁸ D. Das and S. Datta, *Phys. Rev. Lett.* **115**, 131602 (2015).
 - ²⁹ L. Takhtajan, *Physics Letters A* **87**, 479 (1982).
 - ³⁰ H. Babujian, *Physics Letters A* **90**, 479 (1982).
 - ³¹ G. V. Uimin, *Zh. Eksp. Fiz. Pis'ma Red.* **12**, 331 (1970).
 - ³² C. K. Lai, *Journal of Mathematical Physics* **15**, 1675 (1974).
 - ³³ B. Sutherland, *Phys. Rev. B* **12**, 3795 (1975).
 - ³⁴ N. Kawakami, *Phys. Rev. B* **46**, 3191 (1992).
 - ³⁵ M. Greiter, *Mapping of Parent Hamiltonians: from Abelian and non-Abelian Quantum Hall States to Exact Models of Critical Spin Chains* (Springer Tract of Modern Physics,

- 2011).
- ³⁶ R. Thomale, S. Rachel, P. Schmitteckert, and M. Greiter, *Phys. Rev. B* **85**, 195149 (2012).
- ³⁷ O. M. Sule, H. J. Changlani, I. Maruyama, and S. Ryu, *Phys. Rev. B* **92**, 075128 (2015).
- ³⁸ W. Marshall, *Proc. R. Soc. Lond. A* **232**, 48 (1955).
- ³⁹ In general, the basis we are using is non-orthonormal. However, there are special points, including the ground states of the SU(3) Haldane-Shastry model and the Pfaffian spin chain, where the Jack polynomial structure of the individual eigenstates assures the basis we use is orthonormal and that all the weight is located in one momentum sector. More specifically, all basis states are obtained by “squeezing” operations from a root configuration⁶². For example, the root configuration for the Pfaffian chain is $|2, 0, 2, 0, \dots, 2, 0\rangle$ and the total momentum is $N^2/2$. For all other models considered in this work, a significant portion of the ground state weight is still in the same momentum sector, making it a good approximation to consider the basis we use as orthonormal. We compute the momentum-space ES using all momentum sectors but still assume the total momentum is a good quantum number. In general, we expect the ground state of all critical spin chains described by an $SU(N)_k$ WZW field theory to have a significant amount of their weight in one momentum-sector.
- ⁴⁰ D. Schuricht and M. Greiter, *Phys. Rev. B* **73**, 235105 (2006).
- ⁴¹ R. Thomale, D. Schuricht, and M. Greiter, *Phys. Rev. B* **75**, 024405 (2007).
- ⁴² B. I. Halperin, *Helv. Phys. Acta* **56**, 75 (1983).
- ⁴³ E. Ardonne and K. Schoutens, *Phys. Rev. Lett.* **82**, 5096 (1999).
- ⁴⁴ E. Ardonne and N. Regnault, *Phys. Rev. B* **84**, 205134 (2011).
- ⁴⁵ R. Thomale, B. Estienne, N. Regnault, and B. A. Bernevig, *Phys. Rev. B* **84**, 045127 (2011).
- ⁴⁶ We define entanglement weight to be the ratio of the sum of a set eigenvalues of ρ_A to the sum of eigenvalues of ρ_A . For example, for the universal entanglement weight, the set of eigenvalues used are the universal entanglement levels below the EG.
- ⁴⁷ I. Affleck and F. D. M. Haldane, *Phys. Rev. B* **36**, 5291 (1987).
- ⁴⁸ A. E. B. Nielsen, J. I. Cirac, and G. Sierra, *Journal of Statistical Mechanics: Theory and Experiment* **2011**, P11014 (2011).
- ⁴⁹ F. Michaud, F. Vernay, S. R. Manmana, and F. Mila, *Phys. Rev. Lett.* **108**, 127202 (2012).
- ⁵⁰ M. Greiter and R. Thomale, *Phys. Rev. Lett.* **102**, 207203 (2009).
- ⁵¹ B. Scharfenberger, R. Thomale, and M. Greiter, *Phys. Rev. B* **84**, 140404 (2011).
- ⁵² M. Milovanović and N. Read, *Phys. Rev. B* **53**, 13559 (1996).
- ⁵³ The finite effects in the ES counting as well as the perspective from root partition monomials in momentum space show that the $(N, N_A) = (12, 6)$ sector corresponds to the $\mathbb{1}$ branch and the $(N, N_A) = (12, 7)$ sector to the Ψ branch. The σ branch is resolved by the ES analysis related to the ground state of (14) for N odd³⁶.
- ⁵⁴ G. Moore and N. Read, *Nuclear Physics B* **360**, 362 (1991).
- ⁵⁵ P. Calabrese and J. Cardy, *Journal of Statistical Mechanics: Theory and Experiment* **2004**, P06002 (2004).
- ⁵⁶ More specifically, the continuum limit of the distribution of entanglement levels is only approached for system sizes of 1000 or more¹⁴ and the width of this boundary CFT scales as $\ln L$ indicating this method is limited to large system sizes¹⁵.
- ⁵⁷ N. Andrei and H. Johannesson, *Physics Letters A* **104**, 370 (1984).
- ⁵⁸ H. Johannesson, *Nucl. Phys.* **B270**, 235 (1986).
- ⁵⁹ F. C. Alcaraz and M. J. Martins, *Journal of Physics A: Mathematical and General* **23**, L1079 (1990).
- ⁶⁰ M. J. Martins, *Phys. Rev. Lett.* **65**, 2091 (1990).
- ⁶¹ H. Johannesson, *Journal of Physics A: Mathematical and General* **21**, L1157 (1988).
- ⁶² B. A. Bernevig and F. D. M. Haldane, *Phys. Rev. Lett.* **100**, 246802 (2008).